Biophysical Chemistry 195 (2014) 43–48

Contents lists available at ScienceDirect

Biophysical Chemistry

journal homepage: http://www.elsevier.com/locate/biophyschem

Interfacial binding and aggregation of lamin A tail domains associated with Hutchinson–Gilford progeria syndrome

Agnieszka Kalinowski [a], Peter N. Yaron [b], Zhao Qin [c], Siddharth Shenoy [d], Markus J. Buehler [c], Mathias Lösche [a,c,*], Kris Noel Dahl [a,b,*]

[a] Department of Biomedical Engineering, Carnegie Mellon University, 5000 Forbes Ave., Pittsburgh, PA 15213, United States
[b] Department of Chemical Engineering, Carnegie Mellon University, 5000 Forbes Ave., Pittsburgh, PA 15213, United States
[c] Department of Civil and Environmental Engineering, MIT, 77 Massachusetts Avenue, Cambridge, MA 02139, United States
[d] Department of Physics, Carnegie Mellon University, 5000 Forbes Ave., Pittsburgh, PA 15213, United States

HIGHLIGHTS

- We measured the protein–membrane binding of lamin tail domains.
- Farnesylated lamins bind in the presence of Mg^{2+} and Ca^{2+}.
- Electrostatics also promote protein–membrane binding.
- Disease causing lamin mutants both bind membranes and aggregate at the interface.

GRAPHICAL ABSTRACT

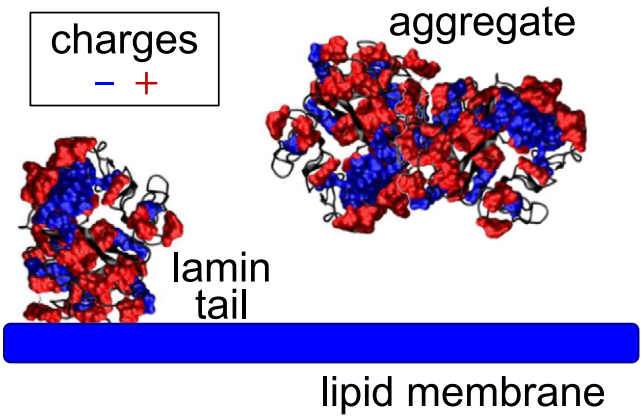

ARTICLE INFO

Article history:
Received 14 March 2014
Received in revised form 28 July 2014
Accepted 3 August 2014
Available online 23 August 2014

Keywords:
Lamin A
Farnesylation
Hutchinson–Gilford progeria syndrome
Protein–membrane

ABSTRACT

Hutchinson–Gilford progeria syndrome is a premature aging disorder associated with the expression of Δ50 lamin A (Δ50LA), a mutant form of the nuclear structural protein lamin A (LA). Δ50LA is missing 50 amino acids from the tail domain and retains a C-terminal farnesyl group that is cleaved from the wild-type LA. Many of the cellular pathologies of HGPS are thought to be a consequence of protein–membrane association mediated by the retained farnesyl group. To better characterize the protein–membrane interface, we quantified binding of purified recombinant Δ50LA tail domain (Δ50LA-TD) to tethered bilayer membranes composed of phosphatidylserine and phosphocholine using surface plasmon resonance. Farnesylated Δ50LA-TD binds to the membrane interface only in the presence of Ca^{2+} or Mg^{2+} at physiological ionic strength. At extremely low ionic strength, both the farnesylated and non-farnesylated forms of Δ50LA-TD bind to the membrane surface in amounts that exceed those expected for a densely packed protein monolayer. Interestingly, the wild-type LA-TD with no farnesylation also associates with membranes at low ionic strength but forms only a single layer. We suggest that electrostatic interactions are mediated by charge clusters with a net positive charge that we calculate on the surface of the LA-TDs. These studies suggest that the accumulation of Δ50LA at the inner nuclear membrane observed in cells is due to a combination of aggregation and membrane

* Corresponding authors at: Department of Biomedical Engineering, Carnegie Mellon University, 5000 Forbes Ave., Pittsburgh, PA 15213, United States.
E-mail addresses: quench@cmu.edu (M. Lösche), krisdahl@cmu.edu (K.N. Dahl).

http://dx.doi.org/10.1016/j.bpc.2014.08.005

association rather than simple membrane binding; electrostatics plays an important role in mediating this association.

1. Introduction

Many human diseases are caused by mutations that alter protein structure and thereby function. In most cases, altered protein structure reduces or eliminates function leading to disease pathology. However, altered protein structures can also lead to interfacial mislocalization, aggregation and other architectural changes. Hutchinson Gilford Progeria Syndrome (HGPS) is an accelerated aging disorder caused by a single base pair mutation (DNA C1824T causes G608G) in *LMNA*, the gene coding for lamin A [1]. The DNA mutation activates a cryptic splice site, and the resulting mutant protein, Δ50 lamin A (Δ50LA), lacks 50 amino acids in its tail domain and as a consequence retains the branched lipid farnesyl group which is added to the C-terminus during posttranslational processing.

HGPS cells show a thicker, stiffer nucleoskeleton with reduced filament exchange [2,3]. The increased association of Δ50LA with the nuclear membrane also affects processes within the nucleus such as DNA repair and transcription [4] as well as transport through nuclear pores [5]. The hyper-association of Δ50LA and other farnesylated lamin mutants with the nuclear membrane is thought to result from the retained lipidation [6], similar to other farnesylated proteins such as Ras and Rho proteins, which show preferential localization to the plasma membrane [7,8]. However, the farnesyl group alone provides only weak protein–membrane association [9], and other factors such as charged amino acid clusters on the protein's membrane-binding interface, a second lipid group or altered binding to transmembrane proteins are likely required for stable protein–membrane association [10].

The primary accepted hypothesis is that the farnesyl lipidation of the Δ50LA is responsible for the pathology of HGPS, including using farnesyl transferase inhibitors as treatment options for patients [11,12]. Here, we suggest that the interaction of LA with the membrane and the hyper-interaction of mutant Δ50LA with the membrane may also be enhanced by electrostatic interactions and aggregation. To this end, we quantify binding of the C-terminal tail domain (TD) of recombinant LA and farnesylated LA variants to synthetic membrane models, sparsely-tethered bilayer lipid membranes (stBLMs). The TDs are spatially distinct from the adjacent rod domains, which are responsible for filament assembly [13,14]. We find that the Δ50LA-TD forms aggregates or complexes at the membrane interface, both in the unfarnesylated and farnesylated forms, whereas the mature wild type LA-TD (m*wt*LA-TD) does not exceed a monolayer of protein at the membrane interface. Thus, the studies of a well-defined synthetic model system reported here suggests a mechanism by which Δ50LA may trigger the formation of a thicker, [3] stiffer [2] nucleoskeleton with altered microdomain structures [2] that accumulate and resist proteolysis [15].

2. Experimental section

2.1. Protein expression, purification and modification

Δ50LA-TD and m*wt*LA-TD were expressed and purified from recombinant plasmids as described previously [16]. In brief, the TD portion (from R386 to the C-terminus) was co-expressed with GST in BL21 Codon-Plus cells (Agilent) at 37 °C. Purification was performed with glutathione magnetic beads (Pierce) and the protein was cleaved enzymatically with proTEV cleavage enzyme (Promega) at 30 °C for 5–7 h. The cleaved protein was further purified by exposure to agarose glutathione beads (Pierce) to remove excess GST. Purified m*wt*LA-TD was dialyzed (Slide-A-Lyzer Dialysis Cassettes) into diH_2O or 50 mM HEPES, 0.5 mM EDTA, pH 7.0.

Δ50LA-TD was modified in vitro to produce fn-Δ50LA-TD [17]. Purified Δ50LA-TD was dialyzed into 50 mM HEPES, pH 7.2, 2 mM $MgCl_2$, 50 mM NaCl and 2 mM DTT, 0.2% octyl-β-D-glucoside, 100 nM farnesyltransferase (Abcam) and 100 μM farnesyl pyrophosphate (MP Biomedicals). The mixture was incubated for >6 h at 37 °C which produced 50% (+/− 10%) farnesylated protein, fn-Δ50LA-TD. Purified proteins were verified for size and farnesylation using liquid chromatography electron spray ionization mass spectroscopy [16], for purity using 14% SDS-PAGE and for concentration using a Bradford assay (Coomassie Plus, Pierce). The modified protein was dialyzed again into buffer (diH_2O, 50 mM NaCl or 50 mM HEPES, 0.5 mM EDTA, pH 7.0).

2.2. Dynamic light scattering

Approximate sizes of protein aggregates were determined using dynamic light scattering (DLS). Purified proteins were concentrated to 1 μM in 100 μL volumes and measured using a Malvern Zetasizer NanoZS in the indicated buffer solutions. Characteristic DLS peaks of $d < 10$ nm were regularly observed under high-salt conditions. Resolution of protein size by DLS under 10 nm is limited. As such, monomer sizes (diameter: ~3 nm for Δ50LA-TD and ~5 nm for m*wt* LA-TD) were estimated from molecular dynamics simulations published previously ([17] and Fig. 2) and used to approximate the expected surface density on the membrane interface.

2.3. Quantification of protein surface charge from simulations

From previously determined replica exchange molecular dynamics simulations of m*wt*LA-TD and Δ50LA-TD [16], we utilized the three-dimensional structures and labeled positive and negative residues. Since there are large regions of intrinsic disorder, we examined the four most representative structures of each protein. Solvent accessible surface area (SASA) values of each residue were calculated in Visual Molecular Dynamics (VMD) [18] using the measure SASA module using a probe radius of 1.4 Å larger than the van der Waals radius of each atom within the residue. The SASA was calculated for all the residues in the four representative structures of each protein and the results are divided into three categories according to the net charge of the residue (positive, negative and neutral). The distributions of each type of charged residues as functions of SASA were therefore statistically computed.

2.4. Preparation of sparsely tethered bilayer lipid membranes (stBLMs)

Acid-washed glass microscope slides (Fisher Scientific) were sputtered (ATC Orion; AJA International) with a layer of chromium (typical thickness: 1 nm) followed by a ~45 nm layer of gold. Sputter conditions were optimized to yield atomically flat gold surfaces (typical large-scale height variations < 3%) [19]. Out of the magnetron recipient, the gold-covered slides were immediately transferred into a 3:7 (mol:mol) 0.2 mM (total concentration) ethanolic solution of Z 20-(Z octadec-9-enyloxy)-3,6,9,12,15,18,22-heptaoxatetracont-31-ene-1-thiol (HC18; a kind gift from Dr. D. J. Vanderah, Institute for Bioscience and Biotechnology Research, Rockville, MD) and β-mercaptoethanol (βME) to form self-assembled monolayers (SAMs) while incubating overnight. After rinsing and drying in a stream of

nitrogen, the SAM-covered slides were immersed into ethanolic solutions containing 1,2-dioleoyl-sn-glycero-3-phosphocholine (DOPC), 1,2-dioleoyl-sn-glycero-3-phospho-L-serine (DOPS), and synthetic cholesterol (Avanti Polar Lipids). Finally, aqueous buffer was flushed rapidly across the substrate [20], which led to the precipitation of a single bilayer to precipitate on the SAM-covered surface. The resulting stBLMs consist of a planar lipid bilayer tethered to the surface through a functionalized lipopolymer, where the thiolated oligo(ethyleneoxide) tethers are interspersed with βME to create a sub-membrane hydration layer. The molecular structure, functionality and in-plane dynamics of such stBLMs have been established with electrochemical impedance spectroscopy, neutron scattering, fluorescence microscopy and fluorescence correlation spectroscopy [21–23].

2.5. Surface Plasmon Resonance spectroscopy

Surface plasmon resonance (SPR) was used to quantify the membrane association of LA-TD on stBLMs by using the gold layer as a medium to support electronic surface plasmons. In a SPR spectrometer of local design [24], purified protein was injected into the buffer adjacent to the bilayer and the change of the minimum angle of the optical reflection from the surface due to plasmon formation was followed over time. The equilibrium values of the SPR signals (time $t \rightarrow \infty$) as a function of protein concentration were determined and fitted to a Langmuir isotherm [24], yielding the apparent dissociation constant, K_D, of the ligand interaction with the surface modeled as a monomeric association. Assuming the optical indices to be $n_{protein} = 1.41$ and $n_{buffer} = 1.33$, and $dn/dc = 0.187$ mL/g [25], addition of a 1 nm layer of protein corresponds to an area density of 5.8 ng/cm^2.

3. Results

3.1. mwtLA-TDs form a single layer on stBLM at low ionic strength

We previously showed the membrane association of the farnesylated Δ50LA-TD, which was expected given the covalently bound lipid group [16]. Here, we examine the membrane association of m*wt*LA-TD, which lacks farnesylation in its mature form within the nucleoskeleton of the cell. Protein was titrated onto a DOPC:DOPS (95:5) stBLM in 50 mM HEPES at pH 7.2, which we refer to as 'low ionic strength' in this paper (Fig. 1). Fitting the data to a Langmuir model yields an equilibrium dissociation constant of $K_D \sim 2$ μM. Based on an estimate of the physical dimension of the TD from molecular dynamics (MD) simulations [16], we calculate the mass density of a single layer of protein on the membrane surface to be ~220 ng/cm^2, which is roughly the coverage of protein on the surface (Fig. 1, gray bar). 50 mM NaCl is sufficient to screen these interactions, and no protein binding is observed under these conditions (data not shown).

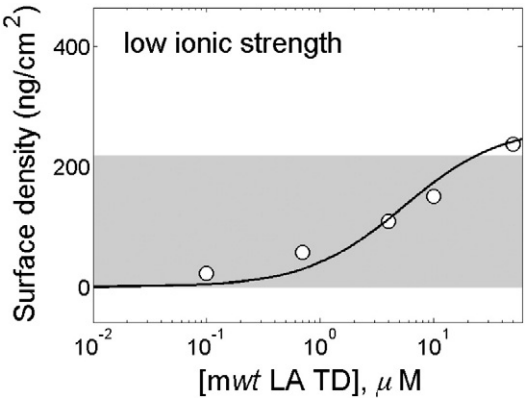

Fig. 1. m*wt*LA-TD associates with charged membranes in low ionic strength buffer but does not exceed monolayer coverage on the interface. Purified m*wt*LA-TD in 50 mM HEPES, pH 7.2 with 0.5 mM EDTA exposed to a stBLM composed of 5% DOPS in DOPC. m*wt*LA-TD does not exceed the mass density expected for a monolayer of protein (~220 ng/cm^2, gray bar).

3.2. Protein electrostatics from simulation

Utilizing simulated protein structures [16] given by molecular dynamics simulations from our previous studies, we found the distribution of the charged residues on the surface of the three-dimensional TD structures as shown in Fig. 2. For both m*wt*LA-TD and Δ50LA-TD, we observe a large cluster of net positive surface charge (Fig. 2, SASA in red) as well as large clusters of both negative and positive residues. We quantitatively determine the distribution of the charged residues in the complex 3D structure by computing the SASA of each residue to understand how the surface area of the TD molecule is occupied by neutral, negative and positive charges (Fig. 2). Using the Gaussian fit, we obtained the mean value and variance of the SASA of each type of residues. We found that for m*wt*LA-TD, the positive residues (326 ± 29 Å^2) have larger SASA than negative (251 ± 21 Å^2) and neutral (220 ± 41 Å^2) residues. This is similar to Δ50LA-TD for positive (317 ± 27 Å^2), negative (248 ± 19 Å^2) and neutral (227 ± 40 Å^2) residues. For comparison, we analyze bovine serum albumin (BSA) and found no such clusters of net charge distribution (Supplemental Fig. 1). BSA as the positive (266 ± 50 Å^2), negative (250 ± 20 Å^2) and neutral residues (231 ± 40 Å^2) have the similar level of SASA. Such analysis, combined with our observation of the charge distributions on the surface of 3D structures, suggests that TD surface are more covered by cationic clusters, which agrees with our hypothesis that protein–membrane association is likely driven by electrostatic interactions between the anionic membrane with cationic clusters on the TD.

3.3. Unfarnesylated Δ50LA-TD binds to stBLMs at low ionic strength and exceeds a monolayer

We examined membrane association of the unfarnesylated Δ50LA-TD under the same conditions as the experiments discussed above. With the lower molecular weight and smaller size [17] of Δ50LA-TD, we estimate that monolayer coverage of the protein should amount to a mass density at the interface of ~140 ng/cm^2, indicated by a gray bar in Fig. 3. However, the experimental data clearly show that the amount of adsorbed protein greatly exceeds the range of mass densities consistent with the formation of a single protein layer. A Langmuir fit yields an apparent dissociation constant $K_D \sim 7$ μM (Fig. 3); we note that the use of a Langmuir model may be inappropriate for a combination of binding and aggregation. Therefore, while both the m*wt*LA-TD and Δ50LA-TD appear to have electrostatic association with stBLMs and show similar affinities in low ionic strength buffer, their overall interaction with the membrane is quite different and may be related to aggregation of Δ50LA-TD at the interface.

3.4. Differences in aggregation of fn-Δ50LA-TD with different divalent cations

To investigate the propensity of the protein for aggregation, the particle sizes of farnesylated fn-Δ50LA-TD in the presence of divalent cations were determined by DLS. We showed previously that membrane association of fn-Δ50LA-TD requires calcium, and calcium induces a conformational change in the protein [17]. Here, we compared fn-Δ50LA-TD aggregation in 50 mM NaCl for a variety of divalent cations present in the nucleus including Ca^{2+}, Mg^{2+}, Mn^{2+} and Zn^{2+} (Fig. 4). Different divalent cations induced two distinct classes of size distributions (Fig. 4). With Ca^{2+} and Mg^{2+}, fn-Δ50LA-TD was stable as a homogeneous distribution of small particles (size <10 nm), consistent with monomeric protein. Conversely, fn-Δ50LA-TD aggregated into μm-sized particles with Mn^{2+} and Zn^{2+} (Fig. 4).

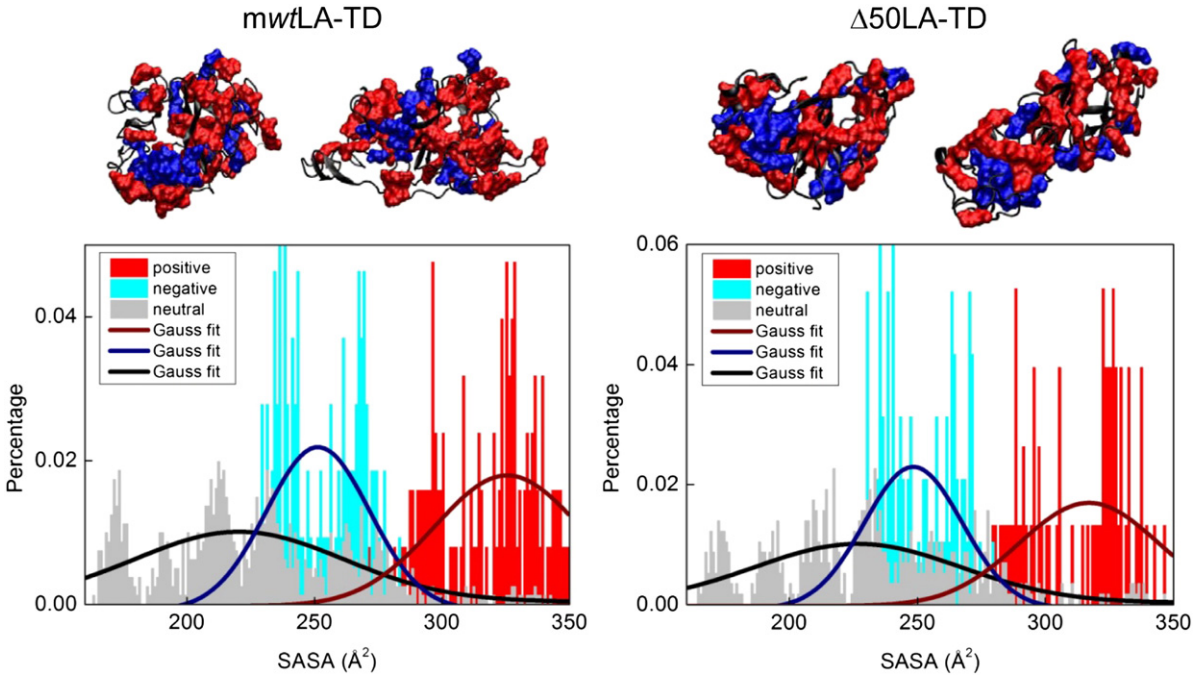

Fig. 2. m*wt*LA-TD and Δ50LA-TD have large clusters of surface charge. From previous molecular dynamics studies, we examine representative structures of the TD sequences with highest probability of appearing. Two sample structures of each protein are shown with charged residues highlighted in red (basic, positive) and blue (acidic, negative) and neutral residues in black. BSA is shown in Supplemental Fig. 1 as a comparison. The solvent accessible surface area (SASA) is then calculated from the three dimensional structure. Both tail domains show a net positive surface with a high percentage of positive residues with a large SASA.

3.5. fn-Δ50LA-TD binds stBLM in the presence of Mg^{2+} and forms interfacial aggregates

To test if membrane binding depends specifically on Ca^{2+} or is also mediated by other divalent cations, we examined if Mg^{2+}, which does not induce protein aggregation in solution (Fig. 4). Indeed, SPR showed that fn-Δ50LA-TD binds to stBLMs in the presence of Mg^{2+} (Fig. 5A) with a similar affinity as in the presence of Ca^{2+}. [17]. However, similar to the unfarnesylated form (Fig. 1), the amount of adsorbed protein exceeds the surface mass density expected for a single protein layer. Rinsing the fully formed protein surface aggregates with 50 mM NaCl and 2 mM $MgCl_2$ (solution buffer) removes minimal protein (Fig. 5B, 2nd and 4th rinse), which suggests that proteins are stably associated. However, incubation of the protein-associated membrane with 10 mM EDTA removes protein, showing that protein association is Mg^{2+}-dependent (Fig. 5B, rinse steps labeled "EDTA").

3.6. Membrane association induces aggregation of fn-Δ50LA-TD

Before membrane exposure fn-Δ50LA-TD is a monomer in Mg^{2+} or Ca^{2+} containing buffer. After membrane exposure, protein size measured by DLS shows formation of large, μm-size aggregates (Fig. 6). In contrast, control samples of protein not exposed to the membrane but held in solution for an extended time were stable as monomers in solution.

4. Discussion

We demonstrated experimentally and with all-atom MD simulations in previous work that Ca^{2+} induces a conformational change in

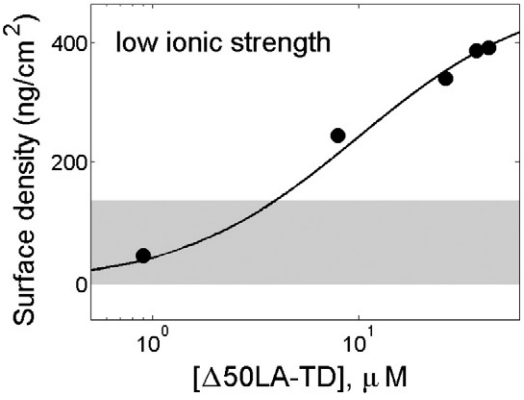

Fig. 3. Unfarnesylated Δ50LA-TD associates with charged membranes in low ionic strength buffer and exceeds the mass density of a protein monolayer on the membrane interface. Purified Δ50LA-TD in 50 mM HEPES, pH 7.2 with 0.5 mM EDTA exposed to a stBLM composed of 5% DOPS in DOPC. The mass density expected for a protein monolayer (~140 ng/cm², gray bar) is exceeded at ~2–3 μM Δ50LA-TD.

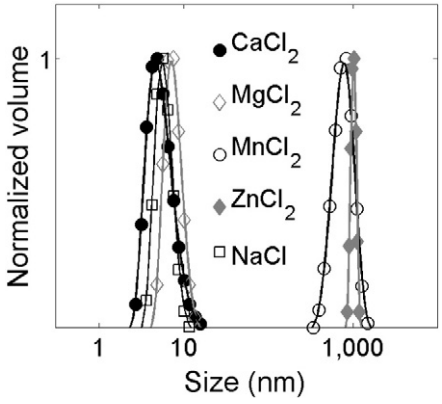

Fig. 4. Aggregation of fn-Δ50LA-TD in buffers with divalent cations. DLS-derived size distributions of 1 μM fn-Δ50LA-TD in 50 mM NaCl and 2 mM divalent cations as indicated. This result suggests that fn-Δ50LA-TD is a monomer in solution without divalent cations or when Ca^{2+} or Mg^{2+} are present in the solvent but aggregates in the presence of Mn^{2+} or Zn^{2+}.

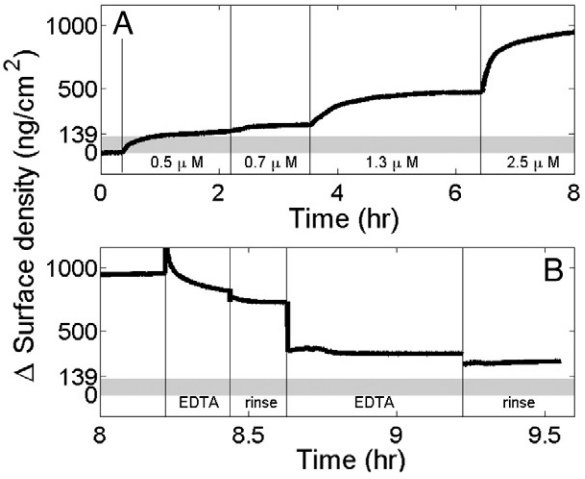

Fig. 5. fn-Δ50LA-TD exceeds monolayer mass density on membrane surfaces in the presence of Mg^{2+} (A) SPR measurements show membrane association of increasing concentrations of fn-Δ50LA-TD in 50 mM NaCl and 2 mM $MgCl_2$ added to an stBLM (30% DOPS in DOPC with 3% cholesterol). The upper bound of area mass density of a complete monolayer of fn-Δ50LA-TD protein is estimated to be 139 ng/cm^2 (gray bar). At 2.5 μM, we observe nearly an order of magnitude higher mass density. (B) fn-Δ50LA-TD dissociates from the membrane surface only minimally when rinsing with EDTA-free buffer (50 mM NaCl and 2 mg $MgCl_2$), but dissociates substantially in the presence of 10 mM EDTA.

the tail domains of prelamin A and Δ50 lamin A that exposes the farnesyl group to the exterior of the protein [17]. Here, we observed that fn-Δ50LA-TD is stable in Mg^{2+} but aggregated in the presence of Mn^{2+} and Zn^{2+}. The significance of fn-Δ50LA-TD aggregation in the presence of Mn^{2+} and Zn^{2+} is unknown, but both ions are found as co-factors for enzymes inside the nucleus [26]. For the full length protein and intermediate filament network, it is possible that Mn^{2+} and Zn^{2+} induced association may help in nucleoskeletal formation after cell division or provide lamin scaffolds for DNA transcription.

As stated in the introduction, the farnesyl group has been hypothesized to be responsible for the pathology of HGPS by increasing membrane association through direct binding. We suggest that it is unlikely that the addition of the 15-carbon farnesyl group alone can alter the localization of the 70 kDa protein substantially and reorganize major parts of the larger nucleoskeletal network. fn-Δ50LA-TD binds to a stBLM in the presence of Mg^{2+} avidly, and its surface density at high concentrations far exceeds that expected for a monolayer, indicating that the protein forms multiple layers on the membrane. Thus, there appears to be a combination of membrane association with aggregation. Table 1 summarizes protein–membrane association under a variety of buffer conditions observed in this and previous works [17].

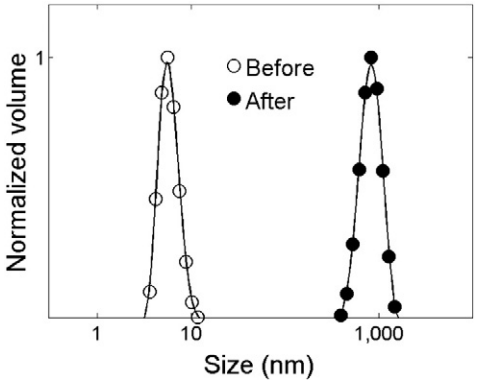

Fig. 6. fn-Δ50LA-TD is aggregated after membrane exposure. Before exposure of fn-Δ50LA-TD to an stBLM, fn-Δ50LA-TD with 2 mM $CaCl_2$, is a monomer in solution, as shown by DLS. After exposure, fn-Δ50LA-TD is aggregated.

Table 1
Summary of protein binding to stBLM in different solution conditions. Protein binding under different buffer conditions where + represents binding that does not exceed a monolayer, ++ represents binding that exceeds a monolayer and – represents no or weak association.

Solution conditions	Δ50LA-TD	fn-Δ50LA-TD	m*wt*LA TD
No salt	++	Aggregation	+
+50 mM NaCl	–	–	–
+2 mM ($CaCl_2$ or $MgCl_2$)	–	++	–

Unfarnesylated Δ50LA-TD and m*wt*LA-TD associate with the membrane only in low ionic strength conditions (50 mM HEPES, pH 7.2 and 0.5 mM EDTA), but no membrane association was observed at 50 mM NaCl. We suggest that a net positive surface charge (30% more positive than negative) of the three-dimensional structure of both Δ50LA-TD and m*wt*LA-TD mediates interaction with the negative membrane (DOPC:DOPS). Both Δ50LA-TD in low ionic strength conditions and fn-Δ50LA-TD in 50 mM NaCl with either Ca^{2+} or Mg^{2+} exceed a monolayer of protein on the surface. Also, these large clusters of both positive and negative charge may lead to aggregation and salt bridging from divalent cations observed with Mn^{2+} and Zn^{2+}. Interestingly, m*wt*LA-TD does not exceed the surface density of a monolayer on the stBLM surface. This surface aggregation difference between Δ50LA-TD and m*wt*LA-TD may be partially responsible for the thickening of the nucleoskeleton observed in patients with HGPS [3]. From the simulations, we observe a slight increase in net positive charge for m*wt*LA-TD over Δ50LA-TD; the monolayer versus multilayer may be a function of the charge differences or from structural differences between the proteins [16].

We conclude from these observations that there is a delicate balance between protein–protein and protein–membrane interactions, as well as a balance between electrostatic interactions and hydrophobic interactions, which depends critically on the magnitude of the Debye screening length, which is approximately 1.4 nm in 50 mM NaCl. Interestingly, this is roughly the length of the farnesyl group, suggesting that the lipidation stays within the electrostatic interaction distance between cationic clusters on the protein and the acidic membrane surface under binding/unbinding fluctuations such that it may easily re-associate with the membrane.

DLS of the protein after membrane exposure indicates that membrane exposure induces protein aggregation. Whether the membrane triggers a protein conformational change is unclear, but it is apparent that the membrane promotes protein–protein interaction and aggregation. The aggregation of the TDs – adsorption beyond a single monolayer and membrane-induced protein aggregation – may correlate with the aggregation potential for the full length form of the protein, Δ50LA. Inside cells, filaments of fn-Δ50LA thicken the nucleoskeleton [3] and can organize into ordered microdomains of filaments at the inner nuclear membrane [2]. Our results suggest that the formation of these thick, ordered filament networks results as much from aggregation of Δ50LA as from a farnesyl-mediated membrane association. Even if unfarnesylated, full length Δ50LA forms tighter in vitro reconstituted structures than the m*wt*LA in vitro [27], likely from the smaller, more stable TD [16]. Furthermore, the membrane-induced aggregation and other patho-physiologic aspects of the non-farnesylated form of Δ50LA-TD (as well as of its farnesylated counterpart) are consistent with the disease-causing nature of the non-farnesylated form of Δ50LA in mice, where expression of nonfarnesylated Δ50LA results in milder cellular and organismal phenotypes of HGPS, which were, however, not completely functional [28].

5. Conclusion

In this work, the membrane affinities of LA-TD and its pathogenic mutants provide insight in the toxic enhancement of Δ50LA with the inner nuclear membrane. We find that both the normal m*wt*LA and

unfarnesylated mutant Δ50LA-TD can associate with charged membranes in low ionic strength buffer, but Δ50LA-TD exceeds a monolayer on the membrane surface. The farnesylated form of Δ50LA-TD binds the membrane strongly at physiological levels of salt in the presence of Ca^{2+} or Mg^{2+}, but membrane association is coupled with aggregation. Zn^{2+} and Mn^{2+}, both found in the nucleus, cause aggregation of fn-Δ50LA-TD in solution.

Supplementary data to this article can be found online at http://dx.doi.org/10.1016/j.bpc.2014.08.005.

Acknowledgments

We acknowledge the help in protein production and purification by Matthew Biegler (CMU MSE) and Kelli Coffey (CMU ChemE) and funding received by K.N.D. (Progeria Research Foundation and NSF CBET — 0954421 CAREER), A.K. (NIH-NIA NRSA F30-AG030905) and M.L. (NIH-NIGMS 1R01-GM101647). M.J.B. and Z.Q. acknowledge support from ONR-PECASE N000141010562 and NIH U01 EB014976.

References

[1] M. Eriksson, et al., Recurrent de novo point mutations in lamin A cause Hutchinson–Gilford progeria syndrome, Nature 423 (6937) (2003) 293–298.
[2] K.N. Dahl, et al., Distinct structural and mechanical properties of the nuclear lamina in Hutchinson–Gilford progeria syndrome, Proc. Natl. Acad. Sci. U. S. A. 103 (27) (2006) 10271–10276.
[3] R.D. Goldman, et al., Accumulation of mutant lamin A causes progressive changes in nuclear architecture in Hutchinson–Gilford progeria syndrome, Proc. Natl. Acad. Sci. U. S. A. 101 (24) (2004) 8963–8968.
[4] S. Reddy, L. Comai, Lamin A, farnesylation and aging, Exp. Cell Res. 318 (1) (2012) 1–7.
[5] A. Busch, et al., Nuclear protein import is reduced in cells expressing nuclear envelopathy-causing lamin A mutants, Exp. Cell Res. 315 (14) (2009) 2373–2385.
[6] J. Barrowman, et al., Human ZMPSTE24 disease mutations: residual proteolytic activity correlates with disease severity, Hum. Mol. Genet. 21 (18) (2012) 4084–4093.
[7] A.D. Cox, et al., Specific isoprenoid modification is required for function of normal, but not oncogenic, Ras protein, Mol. Cell. Biol. 12 (6) (1992) 2606–2615.
[8] M.D. Resh, Trafficking and signaling by fatty-acylated and prenylated proteins, Nat. Chem. Biol. 2 (11) (2006) 584–590.
[9] J.R. Silvius, F. l'Heureux, Fluorimetric evaluation of the affinities of isoprenylated peptides for lipid bilayers, Biochemistry 33 (10) (1994) 3014–3022.
[10] M.J. Nadolski, M.E. Linder, Protein lipidation, FEBS J. 274 (20) (2007) 5202–5210.
[11] A.E. Rusinol, M.S. Sinensky, Farnesylated lamins, progeroid syndromes and farnesyl transferase inhibitors, J. Cell Sci. 119 (Pt. 16) (2006) 3265–3272.
[12] D.T. Smallwood, S. Shackleton, Lamin A-linked progerias: is farnesylation the be all and end all? Biochem. Soc. Trans. 38 (Pt. 1) (2010) 281–286.
[13] H. Herrmann, R. Foisner, Intermediate filaments: novel assembly models and exciting new functions for nuclear lamins, Cell. Mol. Life Sci. 60 (8) (2003) 1607–1612.
[14] H. Herrmann, et al., Functional complexity of intermediate filament cytoskeletons: from structure to assembly to gene ablation, Int. Rev. Cytol. 223 (2003) 83–175.
[15] P. Scaffidi, T. Misteli, Lamin A-dependent nuclear defects in human aging, Science 312 (5776) (2006) 1059–1063.
[16] Z. Qin, et al., Structure and stability of the lamin A tail domain and HGPS mutant, J. Struct. Biol. 175 (3) (2011) 425–433.
[17] A. Kalinowski, et al., Calcium causes a conformational change in lamin A tail domain that promotes farnesyl-mediated membrane association, Biophys. J. 104 (10) (2013) 2246–2253.
[18] W. Humphrey, A. Dalke, K. Schulten, VMD: visual molecular dynamics, J. Mol. Graph. 14 (1) (1996) 33–38 (27–8).
[19] D.J. McGillivray, et al., Molecular-scale structural and functional characterization of sparsely tethered bilayer lipid membranes, Biointerphases 2 (1) (2007) 21–33.
[20] B.A. Cornell, et al., A biosensor that uses ion-channel switches, Nature 387 (6633) (1997) 580–583.
[21] S. Shenoy, et al., In-plane homogeneity and lipid dynamics in tethered bilayer lipid membranes (tBLMs), Soft Matter 2010 (6) (2010) 1263–1274.
[22] I.K. Vockenroth, et al., Stable insulating tethered bilayer lipid membranes, Biointerphases 3 (2) (2008) FA68.
[23] G. Valincius, et al., Enzyme activity to augment the characterization of tethered bilayer membranes, J. Phys. Chem. B 110 (21) (2006) 10213–10216.
[24] S. Shenoy, et al., Membrane association of the PTEN tumor suppressor: molecular details of the protein–membrane complex from SPR binding studies and neutron reflection, PLoS One 7 (4) (2012) e32591.
[25] J.A. De Feijter, J. Benjamins, F.A. Veer, Ellipsometry as a tool to study the adsorption behavior of synthetic and biopolymers at the air–water interface, Biopolymers 17 (7) (1978) 1759–1772.
[26] L.M. Neri, et al., Spatial distribution of lamin A and B1 in the K562 cell nuclear matrix stabilized with metal ions, J. Cell. Biochem. 75 (1) (1999) 36–45.
[27] P. Taimen, et al., A progeria mutation reveals functions for lamin A in nuclear assembly, architecture, and chromosome organization, Proc. Natl. Acad. Sci. U. S. A. 106 (49) (2009) 20788–20793.
[28] S.H. Yang, et al., Progerin elicits disease phenotypes of progeria in mice whether or not it is farnesylated, J. Clin. Invest. 118 (10) (2008) 3291–3300.